31st Annual International Conference of the IEEE EMBS
Minneapolis, Minnesota, USA, September 2-6, 2009

A Fully Flexible Stimulator using 65 nm CMOS Process for 1024-electrode Epi-retinal Prosthesis

N. Tran, J. Yang, S. Bai, D. Ng, M. Halpern, D. B. Grayden, E. Skafidas, and I. Mareels

Abstract—**This paper presents a fully flexible stimulator using 65 nm CMOS process for a 1024-electrode epi-retinal prosthesis. The stimulator can select any number of electrodes at any time and also supports both mono-polar and multi-polar stimulation. Furthermore, the stimulator supports a wide range of stimulus parameters. A novel feature is that the electrode driver operates in an alternately pull-push manner, which helps reduce headroom voltage while guaranteeing charge balance at the active electrode. The use of positive supplies instead of both positive and negative supplies simplifies CMOS circuit design. The current distribution between two nearby simultaneously active electrode groups was investigated and measurement result showed a maximum current crosstalk of 8%.**

I. Introduction

Retinal prostheses are being developed worldwide to help restore partial vision in patients suffering from eye diseases such as retinitis pigmentosa (RP) or age-related macular degradation (AMD) [1-4]. Trials in humans with small numbers of electrodes showed that electrical stimulation of ganglion cells can evoke the perception of light in the patients [2, 5]. It has been suggested that a minimum number of 600-1000 electrodes will be needed for the blind to read large-sized text, navigate a room unaided, and recognize faces [6-9].

As the number of electrodes increases to 1000, the controlling circuit becomes quite complicated and needs to be carefully designed so that it can drive the electrode array effectively with low power consumption. This is critical when the power is transferred wirelessly. In addition, the microchip must be compact enough to be implanted on the retina surface. Recent work [2] revealed low thresholds of light perception with the use of three-dimensional electrodes ensuring close contact to the ganglion cells, which makes it possible to use lower stimulus voltage than previously for flat electrodes [1, 4]. Therefore, it is vital and possible to use small scale CMOS process for implementing this microchip to realize a high level of circuit integration as well as low power consumption in a small single chip. We are developing a prototype microchip using 65 nm CMOS process for a 1024-electrode epi-retinal prosthesis that uses penetrating electrodes to stimulate the ganglion cells. As a prototype chip, it is necessary that the chip should be as flexible as possible in terms of the capability of choosing any active electrode and any number of electrodes to stimulate simultaneously, or choosing which electrodes to be return ones, and the capability of supplying wide ranges of stimulus current as well as stimulus pulse duration.

This paper presents the stimulation controller and electrode drivers, which are two key blocks in determining the flexibility of the whole retinal prosthesis. Measurement result of current distribution between two nearby simultaneously active electrode groups is also presented.

Manuscript received on April 7 2009. This work was supported by Australia's ICT Research Centre of Excellence (NICTA) and Bionic Vision Australia (BVA).

N. Tran, J. Yang, S. Bai, E. Skafidas, D. Ng, M. Halpern, and D. B. Grayden are with Australia's ICT Research Centre of Excellence (NICTA), Victoria Research Laboratory, Parkville, VIC 3010, Australia. N. Tran, J. Yang, S. Bai, D. B. Grayden, and I. Mareels are with the Department of Electrical and Electronic Engineering, The University of Melbourne, Parkville, VIC 3010, Australia. D. B. Grayden is also with the Bionic Ear Institute, East Melbourne, VIC 3002, Australia.

II. Methods

A. Architecture

A bionic eye includes a camera for image capture and a processor to process the captured image and send it to an implant device where the image data is converted into electrical current to stimulate the retina, which is then translated back to a representation of the captured image by the visual cortex. The implant device wirelessly receives the image data and power for its operation through inductive coupling links. Fig. 1 shows the architecture of the implant device, which consists of a power recovery unit and its power coil, a transceiver and its data coil, a baseband controller, a stimulation controller, diagnostic circuitry, electrode drivers, and an electrode array. This work focuses on the stimulation controller and the electrode drivers, which use data from the transceiver to drive the electrode array.

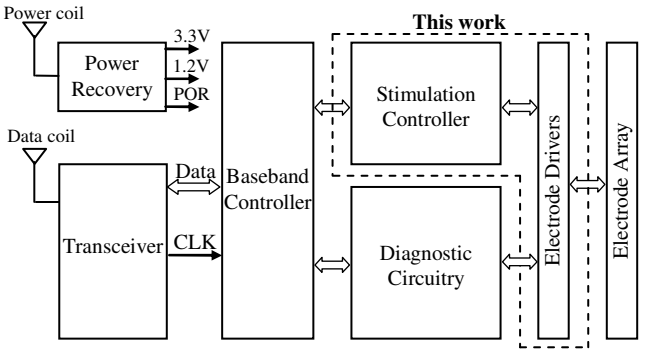

Fig. 1. Architecture of the implant device. This work focuses on the stimulation controller and the electrode drivers.

B. Stimulation strategies

The bi-phasic current pulse has been widely used as a

desired means of stimulating retina tissue whilst ensuring charge balance at the electrodes [1-4]. The light brightness may be represented by stimulus current amplitude [10] or possibly by rate of stimulation [11]. The stimulator in this work can support both of these two stimulation methods. Fig. 2 shows the waveforms of the two stimulation approaches. In Fig. 2a, the stimulus current amplitude is variable to represent the brightness while other parameters such as current pulse widths, inter-phase delay and stimulus rate (refresh rate) are fixed. To achieve flicker-free vision, the refresh rate is chosen to be 60 Hz [10]. Meanwhile, in Fig. 2b, all parameters of the stimulus current are fixed with smaller stimulus pulse duration (200-250 Hz), and the brightness is determined by the number of stimulus pulses (rate coding) in one refresh period.

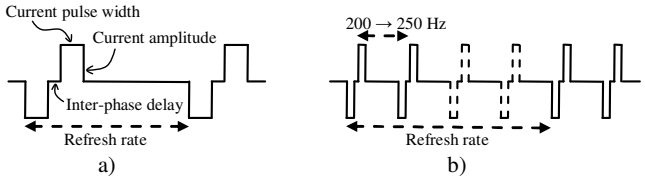

Fig. 2. Two stimulation approaches to represent phosphene brightness. a) Using current amplitude, b) Using rate of stimulation.

The selection of return electrodes is of importance, especially when simultaneous stimulation is needed as crosstalk between simultaneously active currents may happen and reduce image resolution. Common return electrode has been employed [1] but the crosstalk issue has not yet been addressed. A hexagonal mosaic of electrodes surrounding the active electrode has been used as return electrodes and showed good isolation in simultaneous stimulation [4]. However, the fact that only 14 out of 98 electrodes could be simultaneously active makes the system less flexible. Moreover, the push-pull configuration in this system consumes more headroom voltage, which is critical when low stimulus voltage is used.

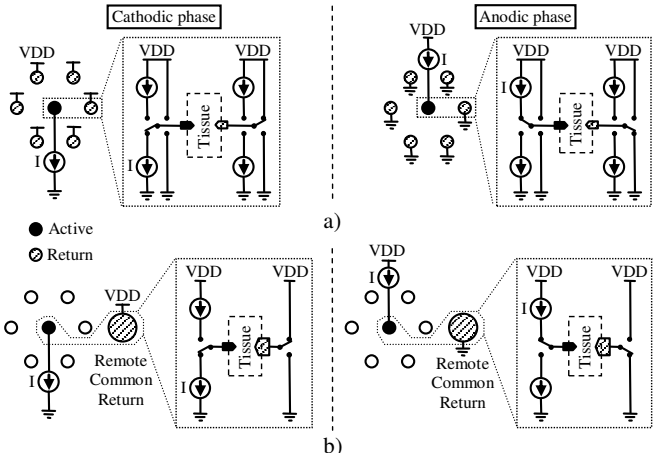

Fig. 3. Two approaches of selecting return electrodes. a) Surrounding return, b) Common return.

In this work, each electrode is driven by one driver, which can connect the electrode to either a current sink or a current source or VDD or GND. An active electrode is first connected to a current sink, and then a current source to generate bi-phasic stimulus current, while its return electrode(s) is connected to VDD, and then GND, respectively. This alternately pull-push manner makes the stimulus current at the active electrode controllable and also consumes less headroom voltage as only one current sink or source is used at a time. In addition, the ability to switch return electrodes between VDD and GND makes it possible to use only a single supply rail, which is preferable in CMOS circuit design. A similar driver has been proposed in [12] but it was followed by a demultiplexer, which not only consumes more headroom voltage but also reduces the flexibility in choosing active electrodes. Fig. 3 shows two main approaches of choosing return electrodes supported by the microchip: surrounding return and common return. The common return electrode can be placed at the back of the eye ball or can be just a large pad on the chip which is exposed to the vitreous humor.

C. Stimulation controller

Stimulation controller shown in Fig. 4 is the most important block in this work as it controls the stimulation operation. The operation of the stimulation controller can be divided into two phases: configuration and stimulation. In configuration phase, the input data goes into a configuration unit where all pre-defined stimulus parameters are set such as brightness representing mode, return configuration, sequence of stimulation, bias voltages. In stimulation phase, input data goes into current amplitude data register (or rate coding data register in case of rate coding mode) from which the electrode drivers read data out to drive electrodes. Image data is written into data registers at an update rate of about 24 Hz (as standard video frame rate) while the data is read out for stimulation at a refresh rate of 60 Hz for flicker-free vision. This separation of update rate and refresh rate helps reduce data transmission bandwidth. The controller mainly operates in stimulation phase unless the pre-defined stimulus parameters need to be reset.

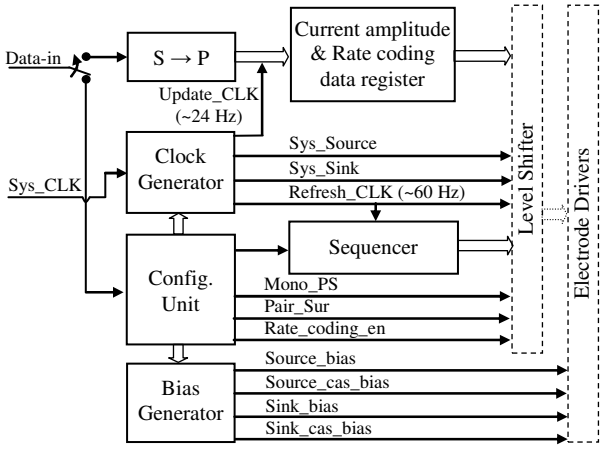

Fig. 4. Architecture of the stimulation controller.

The following three sections describe the sequencer, electrode driver, and level shifter. The sequencer and the electrode driver are two most important blocks determining the flexibility of the system while the level shifter is one of

the most used sub-circuits in the chip.

D. Sequencer

To stimulate 1024 electrodes at a refresh rate of 60 Hz (16.67 ms) with the whole stimulus pulse duration of 1 ms, 64 electrodes must be simultaneously activated (16 time slices x 64 electrodes). It is necessary that the selection of those 64 electrodes must be as flexible as possible to investigate all possible stimulation patterns. The sequencer including 1024 16-bit shift registers as shown in Fig. 5 can activate any number of electrode drivers at any time slice. Once data representing sequence of stimulation has been shifted in, the 16-bit shift registers keep circulating to periodically activate the electrode drivers. This flexible architecture is really useful as the prototype stimulator needs as many functions as possible. For example, the refresh rate is kept at 60 Hz but the whole stimulus current pulse duration is now increased to 2 ms to allow more charge to be injected into tissue, which results in only 8 time slices and, therefore, 128 electrode drivers need to be activated in each time slice. This is easily done by the sequencer by activating 128 out of 1024 registers at two consecutive time slices while still keeping the refresh (circulate) rate at 60Hz.

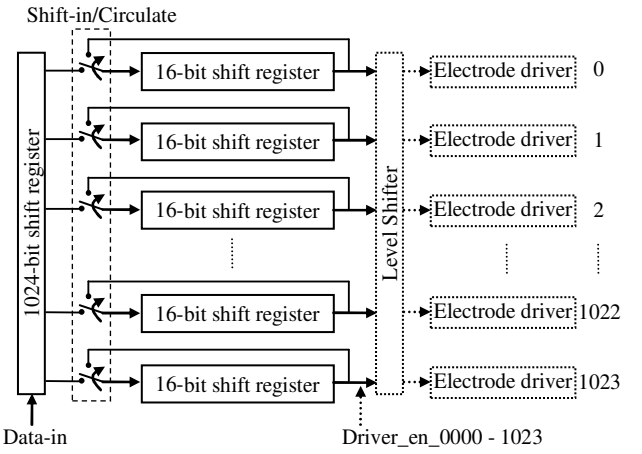

Fig. 5. Architecture of the sequencer which consists of 1024 16-bit shift registers and one 1024-bit shift register.

E. Electrode driver

The electrode driver shown in Fig. 6 can satisfy all the functions that the stimulation controller requires. The driver is activated by the sequencer via 1024 16-bit shift registers. The rate coding mapping unit bypasses the system source and system sink signals when the controller is in current amplitude mode. Otherwise, it maps these two signals with the corresponding rate coding data to generate the source enable and sink enable for its electrode driver. In common return mode, all the logic on the right disables the switches to VDD and GND making the electrode serve as active electrode only, while in surrounding return mode, these two switches are enabled so that the electrode driver can drive the electrode as an active or return one.

The driver also has the ability of choosing only one return electrode instead of all surrounding return electrodes in case current crosstalk is found to be small when electrodes are activated far apart from each other.

The electrode drivers are implemented using thick-oxide transistors in 65 nm CMOS process which can tolerate a voltage up to 3.3V.

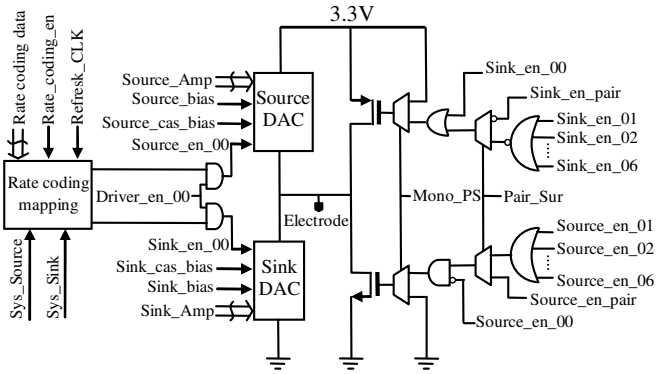

Rate_coding_en = 1: rate coding mode
Rate_coding_en = 0: current amplitude mode
Source_en_xx = 1: switch to current source
Sink_en_xx = 1: switch to current sink
Mono_PS = 1: Mono-return (common return)
Mono_PS = 0: Pair or surrounding return
Pair_Sur = 1: Pair return
Pair_Sur = 0: Surrounding return
* Sink_en_pair is one of Sink_en_01-06 (similar to Source_en_pair)

Fig. 6. Schematic of the electrode driver.

F. Level shifter

All the digital circuits in the implant are implemented using thin-oxide transistors, which need low supply voltage to achieve low power consumption, while the electrode drivers are implemented using thick-oxide transistors to tolerate high supply voltage, which is needed to generate high stimulus current. Therefore, level shifters are needed to shift controlling signals from 1.2V up to 3.3V to drive the electrode drivers. Because all the controlling signals and data interfacing with the electrode drivers need to be shifted up, the level shifter must be as simple as possible. In this work, the level shifter is implemented using a pair of inverters, one of which uses thin-oxide transistors while the other uses thick-oxide transistors as shown in Fig. 7. By choosing appropriate width/length ratio, the inverting threshold of the thick-oxide inverter can be reduced down to 0.6V which is at the middle of the digital signal from the controller.

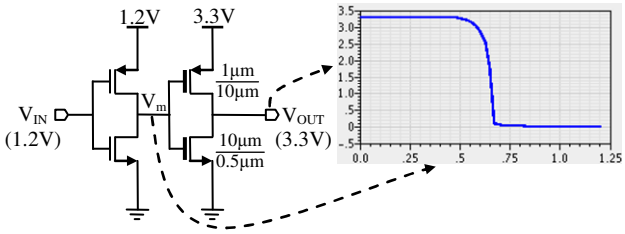

Fig. 7. Schematic of the level shifter.

III. Results

A. Current distribution measurement results

In simultaneous stimulation, current crosstalk is critical as it can reduce image resolution. For current project, penetrating electrodes using boron doped diamond are being used to ensure close contact to the ganglion cells, and they are currently under development. Therefore, for investigating

current distribution, flat Au-Cu electrodes are used instead. Fig. 8 shows the setup to investigate the current distribution. Electrodes with diameter of 250 µm are arranged in hexagonal mosaic with gap between any two electrodes of 1 mm. The electrode array is dipped in saline solution to allow stimulus currents to flow. Two nearby electrode groups each consisting of seven electrodes (one center acting as active electrode and six surroundings acting as return electrodes) are stimulated. Two currents are injected into two central electrodes, and then two currents returning from two corresponding return electrode groups are measured to see how the two inject currents are distributed. Ideally, in each electrode group, the return current should be the same as the inject one, but this is not the case when crosstalk occurs.

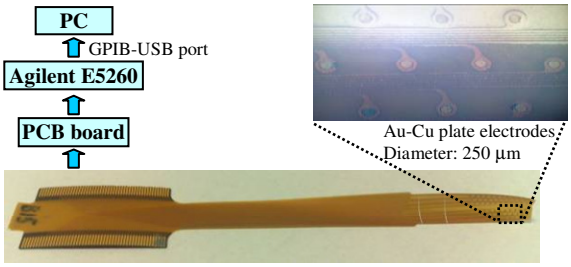

Fig. 8. Strip Au-Cu electrode array and current distribution measurement setup. The strip electrode array consists of an array of 84 electrodes placed in 6 lines and a connector to be connected to a PCB board which draws stimulus current from Agilent E5260. A PC is used to control Agilent E5260 via a GPIB-USB cable.

The current distribution result in Fig. 9 shows a maximum current crosstalk of 8%, which is not too high and can be reduced when stimulating with the configuration in which two nearby electrodes are never activated at the same time.

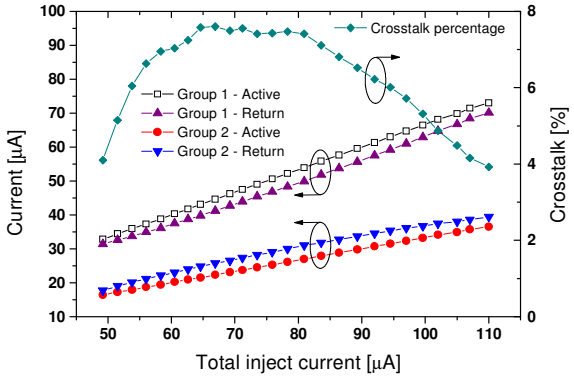

Fig. 9. Measurement result of current distribution between two groups of electrode each of which consists of 1 active electrode and 6 surrounding return electrodes, two groups are next to each other. Current in group 1 is from 30 to 70 µA while that of group 2 is from 15 to 35 µA. Part of current from group 1 returning via group 2 causes current crosstalk.

B. Circuit area estimation

Since the system is currently under development, an estimation of circuit area is necessary to make sure the whole system is feasible in terms of silicon area. A Set/Clear D-FF which is the most area-consuming element in the controller besides the electrode driver has been laid out. Due to the small feature size of 65 nm CMOS process, the D-FF area is only 24 µm^2 making the sequencer an area of about 0.42 mm^2, which is quite small compared to the total chip area of 5x5 mm^2.

IV. Discussions

As a prototype, the controller has been designed with as many options as possible. The power consumption of the controller and electrode drivers as well as the whole implant device needs to be investigated to check the feasibility in term of power consumption. The current crosstalk can be reduced by setting the simultaneously active electrodes far away from each other, which can be done by cleverly choosing 64 out of 1024 electrodes.

V. Conclusions

A prototype microchip for fully flexible 1024-electrode epi-retinal prosthesis is under development. Detailed circuit designs of the stimulation controller and electrode drivers were presented and the whole system was shown to be feasible to realize.

References

[1] M. Sivaprakasam, L. Wentai, W. Guoxing, J. D. Weiland, and M. S. Humayun, "Architecture tradeoffs in high-density microstimulators for retinal prosthesis," *IEEE Transactions on Circuits and Systems I: Regular Papers,* vol. 52, pp. 2629-2641, 2005.

[2] C. Koch, W. Mokwa, M. Goertz, and P. Walter, "First results of a study on a completely implanted retinal prosthesis in blind humans," *IEEE Sensors,* pp. 1237-1240, 2008.

[3] T. Tokuda, R. Asano, S. Sugitani, Y. Terasawa, M. Nunoshita, K. Nakauchi, T. Fujikado, Y. Tano, and J. Ohta, "In vivo Stimulation on Rabbit Retina using CMOS LSI-based Multi-Chip Flexible Stimulator for Retinal Prosthesis," *EMBS*, pp. 5790-5793, 2007.

[4] Y. T. Wong, N. Dommel, P. Preston, L. E. Hallum, T. Lehmann, N. H. Lovell, and G. J. Suaning, "Retinal Neurostimulator for a Multifocal Vision Prosthesis," *IEEE Transactions on Neural Systems and Rehabilitation Engineering,* vol. 15, pp. 425-434, 2007.

[5] M. S. Humayun, J. D. Weiland, G. Y. Fujii, R. Greenberg, R. Williamson, J. Little, B. Mech, V. Cimmarusti, G. Van Boemel, G. Dagnelie, and E. de Juan, "Visual perception in a blind subject with a chronic microelectronic retinal prosthesis," *Vis. Res.,* vol. 43, pp. 2573-2581, 2003.

[6] K. Cha, K. W. Horch, R. A. Normann, and D. K. Boman, "Reading speed with a pixelized vision system," *J. Opt. Soc. Am. A,* vol. 9, pp. 673-677, 1992.

[7] K. Cha, K. W. Horch, and R. A. Normann, "Mobility performance with a pixelized vision system," *Vis. Res.,* vol. 32, pp. 1367-1372, 1992.

[8] K. Cha, K. Horch, and R. Normann, "Simulation of a phosphene-based visual field: Visual acuity in a pixelized vision system," *Annals of Biomedical Engineering,* vol. 20, pp. 439-449, 1992.

[9] J. S. Hayes, V.T. Yin, D. Piyathaisere, J. D. Weiland, M. S. Humayun, G. Dagnelie, "Visually Guided Performance of Simple Tasks Using Simulated Prosthetic Vision," *Artificial Organs,* vol. 27, pp. 1016-1028, 2003.

[10] M. S. Humayun, E. de Juan Jr, J. D. Weiland, G. Dagnelie, S. Katona, R. Greenberg, and S. Suzuki, "Pattern electrical stimulation of the human retina," *Vision Research,* vol. 39, pp. 2569-2576, 1999.

[11] D. K. Warland, P. Reinagel, and M. Meister, "Decoding Visual Information From a Population of Retinal Ganglion Cells," *J Neurophysiol,* vol. 78, pp. 2336-2350, 1997.

[12] M. Ghovanloo, and K. Najafi, "A modular 32-site wireless neural stimulation microsystem," *ISSCC*, vol. 1, pp. 226-524, 2004.